

See discussions, stats, and author profiles for this publication at: <https://www.researchgate.net/publication/49783080>

Photochemical and photosensitised reactions involving 1-nitronaphthalene and nitrite in aqueous solution

ARTICLE *in* PHOTOCHEMICAL AND PHOTOBIOLOGICAL SCIENCES · APRIL 2011

Impact Factor: 2.27 · DOI: 10.1039/c0pp00311e · Source: PubMed

CITATIONS

9

READS

44

8 AUTHORS, INCLUDING:



Pratap Reddy Maddigapu

Università degli Studi di Torino

15 PUBLICATIONS 226 CITATIONS

SEE PROFILE



Claudio Minero

Università degli Studi di Torino

326 PUBLICATIONS 8,081 CITATIONS

SEE PROFILE



Davide Vione

Università degli Studi di Torino

264 PUBLICATIONS 3,733 CITATIONS

SEE PROFILE



Mohamed Sarakha

Université Blaise Pascal - Clermont-Ferrand II

71 PUBLICATIONS 927 CITATIONS

SEE PROFILE

Cite this: *Photochem. Photobiol. Sci.*, 2011, **10**, 601

www.rsc.org/pps
PAPER

Photochemical and photosensitised reactions involving 1-nitronaphthalene and nitrite in aqueous solution†

Pratap Reddy Maddigapu,^a Claudio Minero,^a Valter Maurino,^a Davide Vione,^{*a,b} Marcello Brigante,^{*c,d} Tiffany Charbouillot,^{c,d} Mohamed Sarakha^{c,d} and Gilles Mailhot^{c,d}

Received 20th October 2010, Accepted 3rd January 2011

DOI: 10.1039/c0pp00311e

The excited triplet state of 1-nitronaphthalene, 1NN, (³1NN) is able to oxidise nitrite to [•]NO₂, with a second-order rate constant that varies from $(3.56 \pm 0.11) \times 10^8 \text{ M}^{-1} \text{ s}^{-1}$ ($\mu \pm \sigma$) at pH 2.0 to $(3.36 \pm 0.28) \times 10^9 \text{ M}^{-1} \text{ s}^{-1}$ at pH 6.5. The polychromatic quantum yield of [•]NO₂ photogeneration by 1NN in neutral solution is $\Phi_{\text{NO}_2}^{1\text{NN}} \geq (5.7 \pm 1.5) \times 10^7 \times [\text{NO}_2^-] / \{(3.4 \pm 0.3) \times 10^9 \times [\text{NO}_2^-] + 6.0 \times 10^5\}$ in the wavelength interval of 300–440 nm. Irradiated 1NN is also able to produce [•]OH, with a polychromatic quantum yield $\Phi_{\text{OH}}^{1\text{NN}} = (3.42 \pm 0.42) \times 10^{-4}$. In the presence of 1NN and NO₂[−]/HNO₂ under irradiation, excited 1NN (probably its triplet state) would react with [•]NO₂ to yield two dinitronaphthalene isomers, 15DNN and 18DNN. The photonitration of 1NN is maximum around pH 3.5. At higher pH the formation rate of [•]NO₂ by photolysis of NO₂[−]/HNO₂ would be lower, because the photolysis of nitrite is less efficient than that of HNO₂. At lower pH, the reaction between ³1NN and [•]NO₂ is probably replaced by other processes (involving e.g. ³1NN-H⁺) that do not yield the dinitronaphthalenes.

Introduction

1-Nitronaphthalene (1NN) is a genotoxic atmospheric pollutant^{1,2} that is frequently detected in urban air³ despite its fast degradation by direct photolysis.^{4,5} The main sources of 1NN are the direct emission upon combustion processes and the atmospheric nitration of naphthalene.^{6,7} The very fast photolysis of 1NN (half-life time of less than 1 h in the atmosphere)⁸ would make its long-range transport very unlikely. However, significant amounts of 1NN (and of 2NN) have been detected in Antarctic airborne particulate matter.⁹ While the long-range transport from the continents would be excluded, a possible explanation is the gas-phase nitration of naphthalene (probably by [•]NO₃ + [•]NO₂), followed by partitioning of the nitronaphthalenes on the particles at the low temperatures of the Antarctic.¹⁰ Various dinitronaphthalenes have also been detected on the airborne particles in the Antarctic, which is

consistent with a condensed-phase nitration process that takes place *in situ*.⁹

The nitration of the nitroaromatic compounds is an interesting issue; in the case of the formation of 2,4-dinitrophenol, it has been shown that the reaction takes place between the excited mononitrophenols and [•]NO₂.¹¹ The case of excited 1NN is potentially very interesting because of the elevated quantum yield for the formation of the excited triplet state, ³1NN.^{12,13} Moreover, the chemistry of ³1NN is of interest because this species is able to oxidise the halogenide anions to the corresponding radical species, and to produce [•]OH *via* photoinduced generation of O₂^{•−}/HO₂[•] and probably *via* water oxidation.^{14,15} The photosensitised processes in the atmospheric aqueous phase and on particles have recently gained interest because of the role they play in the atmospheric processing of humic-like substances.^{16,17}

This work studies the photochemical reactions that involve 1NN in the presence of nitrite, a major photochemical source of [•]NO₂ in solution.¹⁸ Particular interest is focused on the photoinduced formation of the dinitronaphthalenes. To this purpose, a combination of laser flash photolysis runs and steady-state irradiation experiments was adopted.

Experimental

Reagents and materials

1-Nitronaphthalene (1NN, purity grade 99%), 1,3-dinitronaphthalene (13DNN, 98%), 1,5-dinitronaphthalene (15DNN, 99%), 1,8-dinitronaphthalene (18DNN, 98%), phenol (>99%), 2-nitrophenol (98%) and 4-nitrophenol (>99%) were purchased

^aDipartimento di Chimica Analitica, Università di Torino, Via P. Giuria 5, 10125, Torino, Italy. E-mail: davide.vione@unito.it; Fax: +39-011-6707615; Tel: +39-011-6707838; Web: <http://www.chimicadellambiente.unito.it>

^bCentro Interdipartimentale NatRisk, Università di Torino, Via Leonardo da Vinci 44, 10095, Grugliasco (TO), Italy

^cClermont Université, Université Blaise Pascal, Laboratoire de Photochimie Moléculaire et Macromoléculaire, BP 10448, F-63000, Clermont-Ferrand, France. E-mail: marcello.brigante@univ-bpclermont.fr

^dCNRS, UMR 6505, Laboratoire de Photochimie Moléculaire et Macromoléculaire, F-63177, Aubière, France

† Electronic supplementary information (ESI) available: Effects of nitrite and pH on the decay of ³1NN, pH trend of 1NN transformation rate, effects of 2-propanol and oxygen on the photonitration of 1NN. See DOI: 10.1039/c0pp00311e

from Aldrich, NaNO_2 (>97%) and $(\text{NH}_4)_2\text{Ce}(\text{NO}_3)_6$ (98%) from Carlo Erba, acetonitrile (LiChrosolv gradient grade), 2-propanol (LiChrosolv gradient grade), benzene (for gas chromatography), HClO_4 (70%) and H_3PO_4 (85%) from VWR Int. All reagents were used as received, without further purification. The $\gamma\text{-MnOOH}$ was synthesised following the procedure of Brauer.¹⁹

Irradiation experiments

Two different lamp set-ups were used for the irradiation experiments: a set of three 40 W Philips TL K05 UVA lamps, with emission maximum at 365 nm, and one 100 W Philips TL 01 lamp with emission maximum at 313 nm. The samples (5 mL total volume) were placed into cylindrical Pyrex glass cells (4.0 cm diameter, 2.3 cm height) closed with a lateral screw cap, and were magnetically stirred during irradiation. The incident radiation reached the cells mainly from the top, and the optical path length of the solution was $b = 0.4$ cm. The photon flux incident into the solutions was actinometrically determined using the ferrioxalate method, by taking into account the absorption spectrum of $\text{Fe}(\text{C}_2\text{O}_4)_3^{3-}$ and the variation with wavelength of the quantum yield of Fe^{2+} generation.²⁰ If one knows, as a function of the wavelength, the fraction of radiation absorbed by $\text{Fe}(\text{C}_2\text{O}_4)_3^{3-}$, the quantum yield of Fe^{2+} photoproduction and the shape of the lamp spectrum (*vide infra*), it is possible to use the measured formation rate of Fe^{2+} to fix the value of the incident spectral photon flux density $p^0(\lambda)$. The photon flux

$$P_0 = \int_{\lambda} p^0(\lambda) d\lambda$$

was 4.4×10^{-5} einstein $\text{L}^{-1} \text{s}^{-1}$ for the TL K05 and 3.2×10^{-6} einstein $\text{L}^{-1} \text{s}^{-1}$ for the TL 01 lamp. In both cases the irradiation temperature was around 303 ± 3 K. Fig. 1 reports the emission spectra of the adopted lamps, measured with an Ocean Optics SD 2000 CCD spectrophotometer and normalised to the actinometry results. The Figure also reports the absorption spectra of 1NN, nitrite and HNO_2 , taken with a Varian Cary 100 Scan UV-Vis spectrophotometer.

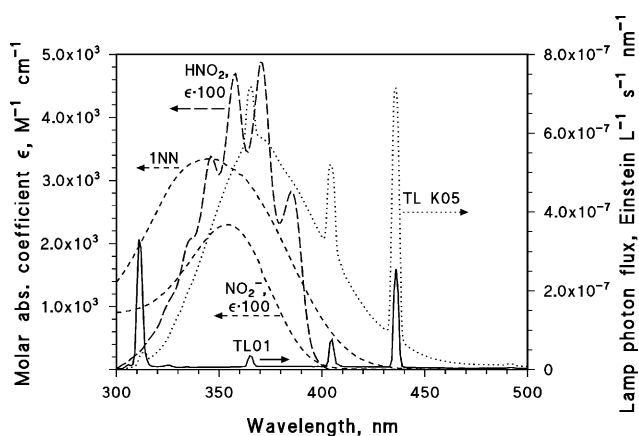


Fig. 1 Emission spectra (spectral photon flux densities $p^0(\lambda)$) of the adopted lamps (TL K05 with emission maximum in the UVA, TL 01 with emission maximum in the UVB). Absorption spectra of 1NN, nitrite and nitrous acid.

Analytical determinations

After irradiation the solutions were allowed to cool for 10–15 min under refrigeration, to minimise the volatilisation of 1NN and, when applicable, that of benzene. Analysis was then carried out by High Performance Liquid Chromatography coupled with UV-Vis detection (HPLC-UV). The adopted Merck-Hitachi instrument was equipped with AS2000A autosampler (100 μL sample volume), L-6200 and L-6000 pumps for high-pressure gradients, Merck LiChrocart RP-C18 column packed with LiChrospher 100 RP-18 (125 mm \times 4.6 mm \times 5 μm), and L-4200 UV-Vis detector (detection wavelength 220 nm). The adopted gradient of CH_3CN : aqueous H_3PO_4 (pH 2.8) was the following: 40:60 for 10 min, then to 60:40 in 1 min and keep for 8 min, back to the initial conditions in 1 min and keep for 8 min. With an eluent flow rate of 1.0 mL min^{-1} the retention times were (min): phenol (2.55), 4-nitrophenol (3.20), 2-nitrophenol (5.15), benzene (8.20), 18DNN (9.06), 15DNN (14.05), 13DNN (16.50), 1NN (17.65). The column dead time was 0.90 min.

Kinetic treatment of the data

The time evolution data of 1NN were fitted with pseudo-first order equations of the form $C_t = C_0 \exp(-kt)$, where C_t is the concentration of 1NN at the time t , C_0 its initial concentration, and k the pseudo-first order degradation rate constant. The initial transformation rate of 1NN is $\text{Rate}_{1\text{NN}} = kC_0$. The time evolution of the intermediates (15DNN and 18DNN from 1NN, phenol from benzene, 2- and 4-nitrophenol from phenol) was fitted with $C'_t = k'_1 C_0 (k_1^d - k_1^d) \exp(-k_1^d t) - \exp(-k_1^d t)$, where C'_t is the concentration of the intermediate at the time t , C_0 the initial concentration of the substrate, k_1^f and k_1^d the pseudo-first order formation and transformation rate constants of the intermediate, respectively, and k_1^d the pseudo-first order transformation rate constant of the substrate. The initial formation rate of the intermediate is $\text{Rate}_i = k_1^f C_0$. The reported errors on the rates were derived from the scattering of the experimental data around the fitting curve, and represent $\mu \pm \sigma$. The reproducibility of repeated runs was around 10–15%.

Radiation absorption calculations

Assume a dissolved species A with concentration c_A and molar absorption coefficient $\epsilon_A(\lambda)$, which is irradiated under a lamp with incident spectral photon flux density $p^0(\lambda)$, in a solution of optical path length b . The spectral photon flux density absorbed by A at the wavelength λ is $p_a^A(\lambda) = p^0(\lambda)[1 - 10^{-\epsilon_A(\lambda)bc_A}]$. The all-wavelength photon flux absorbed by A is $P_a^A = \int_{\lambda} p_a^A(\lambda) d\lambda$.

If the solution contains two light-absorbing species, A and B, the absorbances are additive but the absorbed photon flux densities $p_a^i(\lambda)$ ($i = \text{A or B}$) are not. However, at each wavelength λ the ratio of the spectral photon flux densities would be equal to the ratio of the respective absorbances.²⁴ Therefore, $p_a^A(\lambda) = p_a^B(\lambda)A_A(\lambda)[A_B(\lambda)]^{-1}$, where $A_A(\lambda) = \epsilon_A(\lambda)bc_A$ and $A_B(\lambda) = \epsilon_B(\lambda)bc_B$. It would also be $p_a^A(\lambda) = p_a^{\text{tot}}(\lambda)A_A(\lambda)[A_{\text{tot}}(\lambda)]^{-1}$, where $p_a^{\text{tot}}(\lambda) = p^0(\lambda)(1 - 10^{-A_{\text{tot}}(\lambda)})$ is the total spectral photon flux density absorbed by the solution, and $A_{\text{tot}}(\lambda) = A_A(\lambda) + A_B(\lambda)$.²⁴

A similar expression would also hold for $p_a^B(\lambda)$. For the absorbed photon flux one gets $P_a^i = \int_\lambda p_a^i(\lambda) d\lambda$, where $i = A$ or B .

Laser flash photolysis experiments

A Nd:YAG laser system instrument (Quanta Ray GCR 130-01) operated at 355 nm (third harmonic) with typical energies of 60 mJ (the single pulse was ~ 9 ns in duration) was used to investigate the photosensitised reaction between the excited state of 1NN and nitrite in aqueous solution as a function of pH. Individual cuvette samples (3 mL volume) were used for a maximum of two consecutive laser shots. The transient absorbance at the pre-selected wavelength was monitored by a detection system consisting of a pulsed xenon lamp (150 W), monochromator and a photomultiplier (1P28). A spectrometer control unit was used for synchronising the pulsed light source and programmable shutters with the laser output. The signal from the photomultiplier was digitised by a programmable digital oscilloscope (HP54522A). A 32 bits RISC-processor kinetic spectrometer workstation was used to analyse the digitised signal.

Solutions of both 1NN and NaNO_2 were prepared in Milli-Q water and their stability was regularly checked by means of UV spectroscopy. The decay of the triplet state of 1NN ($^3\text{1NN}$) and the formation of the radical anion ($1\text{NN}^{\cdot-}$) were monitored at 620 and 380 nm, respectively. The pseudo-first order decay and growth constants were obtained by fitting the absorbance vs. time data with single or double exponential equations. The error was calculated as 1σ from the fit of the experimental data; all the experiments were performed at ambient temperature (295 ± 2 K) in aerated solution.

Results

Laser flash photolysis experiments

Fig. 2 shows the transient absorption spectra produced upon LFP excitation (355 nm, 65 mJ) of 1NN (5×10^{-5} M) and NO_2^- (2×10^{-3} M) solution at pH 6.5. Immediately after the laser

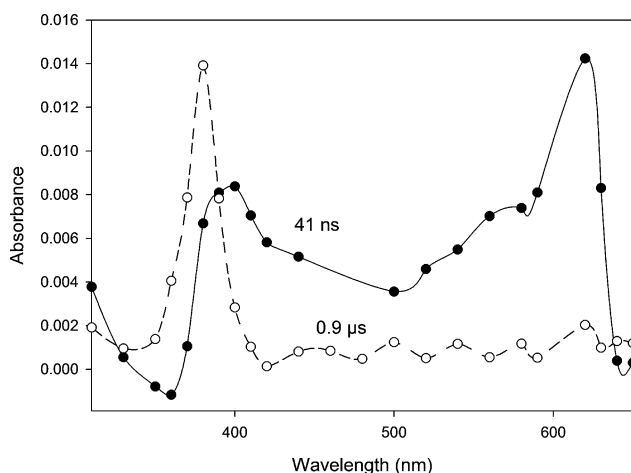


Fig. 2 Transient absorption spectra obtained after 355 nm excitation of 5×10^{-5} M 1NN and 2×10^{-3} M NO_2^- in aqueous solution, at pH 6.5 and $T = 295 \pm 2$ K.

pulse (41 ns), the spectrum of $^3\text{1NN}$ appears with two intense absorptions peaks at 620 and 400 nm, in agreement with previously reported studies.¹⁵ At 0.9 μs , after complete relaxation of the triplet state it can be observed a new intense band centred at 380 nm, which can be attributed mainly to $1\text{NN}^{\cdot-}$.¹⁵ Moreover we noticed that, in the absence of nitrite ions, the maximum absorbance reached at 380 nm (A_{380}) was about 10 times lower than the corresponding A_{620} of $^3\text{1NN}$. Conversely, in the presence of nitrite, the two absorbance values were similar. This finding provides evidence that the addition of nitrite enhances the formation of $1\text{NN}^{\cdot-}$.

Fig. 3A displays the absorbance of $^3\text{1NN}$ monitored at 620 nm, in the presence of different nitrite concentration values at pH 6.5. It is shown that $^3\text{1NN}$ is quantitatively quenched by nitrite and that its pseudo-first order decay constant increases from $\sim 6.0 \times 10^5 \text{ s}^{-1}$ to $3.5 \times 10^7 \text{ s}^{-1}$ in pure water and in the presence of 10 mM NO_2^- , respectively (see insert in Fig. 2A). Regarding the absorbance trend followed at 380 nm reported in Fig. 3B, it is interesting to note the enhancement of the formation rate in the presence of nitrite. The fast triplet state quenching by nitrite ions, which leads, to our knowledge, mainly to the formation of $1\text{NN}^{\cdot-}$, is compatible

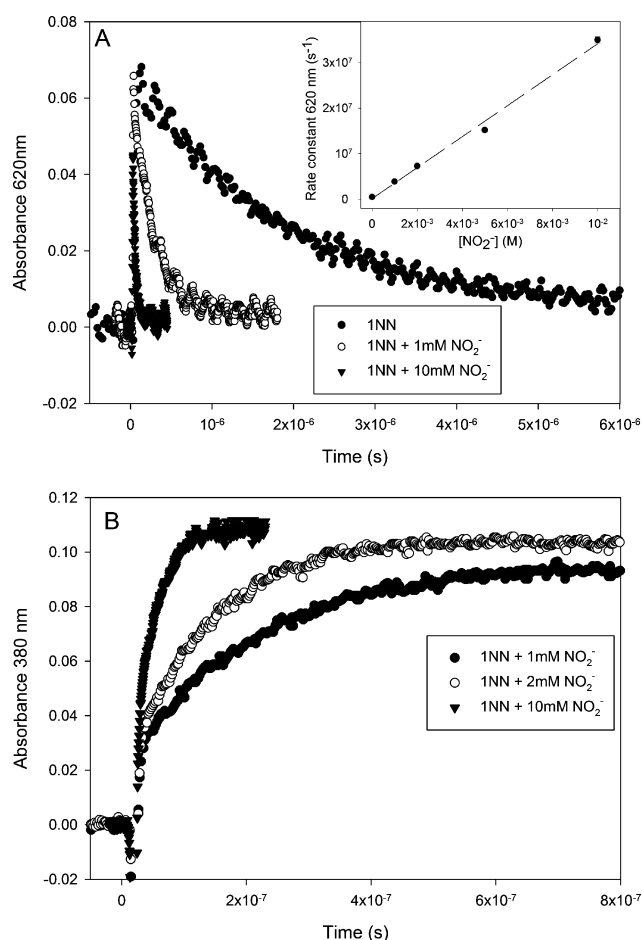
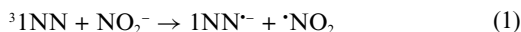


Fig. 3 Transient profiles obtained following LFP (355 nm, 60 mJ) of 1NN (5×10^{-5} M) in aerated solution. (A) Decay at 620 nm corresponding to the triplet state of 1NN ($^3\text{1NN}$) in pure water and with different concentrations of NO_2^- . Insert: pseudo-first order decay constant of $^3\text{1NN}$ followed at 620 nm, in the presence of variable $[\text{NO}_2^-]$. (B) Growth curve of the transient absorbance at 380 nm in the presence of three $[\text{NO}_2^-]$ values.

with the electron-transfer reaction (reaction (1)) between ^3INN and nitrite to yield $\cdot\text{NO}_2$.



Unfortunately we have not been able to directly detect $\cdot\text{NO}_2$ because of its low molar absorption coefficient ($\epsilon_{400\text{ nm}} = 201\text{ M}^{-1}\text{ cm}^{-1}$).²¹

An additional effect of nitrite/ HNO_2 would be their ability to absorb laser radiation at 355 nm, thereby competing with 1NN for the incident photons. To account for this effect, we investigated the variation of the ^3INN absorbance soon after formation as a function of nitrite concentration at different pH values. The corresponding “screen” effect of nitrite on 1NN excitation has been estimated to be linearly dependent on the concentration of nitrite/nitrous acid. For instance, at pH 6.5 the absorbance of ^3INN was decreased by $25 \pm 5\%$ in the presence of 10 mM NO_2^- , compared with pure water. Nevertheless, the competition for irradiance between nitrite and 1NN does not modify the obtained pseudo-first order decay constants, which are not dependent on the triplet state concentration.

Experimental data like those reported in Fig. 3 allowed us to determine the bimolecular rate constants for the quenching of ^3INN by nitrite (Fig. 4). The corresponding trends with $[\text{NO}_2^-]$ of the pseudo-first order rate constants of ^3INN are reported in Fig. ESI1 in the ESI.† The bimolecular rate constant $k_{^3\text{INN},\text{NO}_2^-}$ decreased from $(3.36 \pm 0.28) \times 10^9\text{ M}^{-1}\text{ s}^{-1}$ at pH 6.5 to $(3.56 \pm 0.11) \times 10^8\text{ M}^{-1}\text{ s}^{-1}$ at pH 2.0, showing that the reactivity of ^3INN towards nitrite/ HNO_2 decreases significantly with pH.

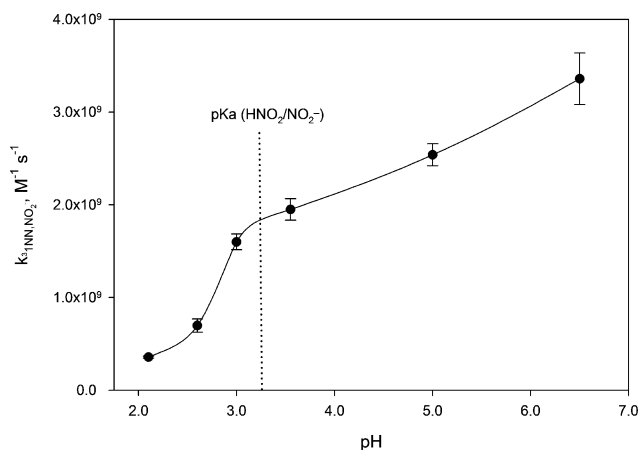


Fig. 4 Bimolecular rate constants for the quenching of ^3INN ($k_{^3\text{INN},\text{NO}_2^-}$) as a function of pH, in aerated aqueous solution at $T = 295 \pm 2\text{ K}$, in the presence of NO_2^- . pH was adjusted with HClO_4 . The dotted vertical line shows the $\text{p}K_a$ of HNO_2 .²⁵

At pH 3.5 and 5.0, the rate constants for the quenching of ^3INN were surprisingly lower than those of formation of the transient monitored at 380 nm. This difference could not be explained on the basis of the electron transfer reaction reported before (reaction (1)). Martins and co-workers¹⁴ reported that pH plays a central role in the electron-transfer reactions from halide ions to ^3INN , via formation of a protonated triplet state ($^3\text{INN-H}^+$). The species $^3\text{INN-H}^+$ is considerably more reactive than ^3INN toward, for example, halides,¹⁵ and a similar effect can also be expected with nitrite/ HNO_2 . However, as reported in a previous study the $\text{p}K_a$

of $^3\text{INN-H}^+$ is ~ 0.66 in water–ethanol solution,¹⁴ and it is difficult to figure out how this species could be able to affect the triplet state reactivity at pH 5. We can argue that part of the 380 nm signal could be attributed to the formation, in addition to $\text{INN}^{\cdot-}$, of unidentified transient species. If this is the case, the kinetic analysis of the 380 nm signal would be next to impossible and no definite conclusion could be derived. Therefore, the following discussion will only be based on the pH trend of the bimolecular rate constant between ^3INN and nitrite, reported in Fig. 4.

Generation of $\cdot\text{NO}_2$ by irradiated 1NN

Steady irradiation was carried out to test the hypothesis that the reaction between ^3INN and nitrite, observed by LFP, really yields $\cdot\text{NO}_2$. Phenol nitration into 2- and 4-nitrophenol was adopted as a probe reaction for the nitrogen dioxide radical, which is a rather effective nitrating agent for phenolic compounds in the aqueous solution.^{22,23} Irradiation took place under the TL 01 lamp, with the purpose of achieving a more efficient excitation of 1NN compared to nitrite (although the two absorption spectra are quite similar in the near UV range, see Fig. 1).

Fig. 5 reports the time evolution of 2- and 4-nitrophenol (2NP, 4NP) upon irradiation of 0.1 mM 1NN, 1 mM phenol, and 10 mM NaNO_2 . The Figure also reports by comparison the time trend of the nitrophenols upon irradiation of phenol and NaNO_2 , without 1NN (in which case $\cdot\text{NO}_2$ is formed by reactions (2) and (3)).¹⁸ The significant enhancement of phenol nitration by 1NN is consistent with the formation of $\cdot\text{NO}_2$ upon reaction (1) between ^3INN and nitrite.

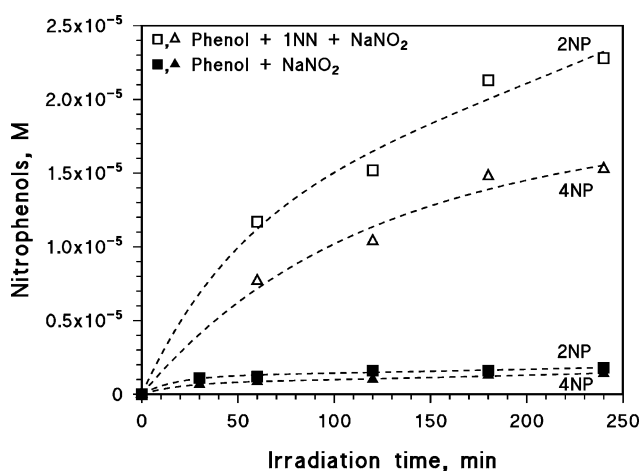
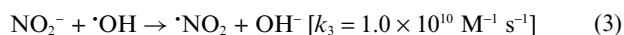
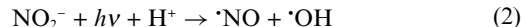


Fig. 5 Time evolution of nitrophenols upon irradiation of 0.1 mM 1NN, 1 mM phenol and 10 mM NaNO_2 (open symbols), and of 1 mM phenol + 10 mM NaNO_2 (solid symbols). Irradiation under the TL 01 lamp, at pH 6.5 and in aerated solution.

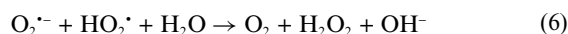
The formation after 4 h irradiation of $\sim 20\text{ }\mu\text{M}$ 2NP and 4NP, with $\text{p}K_a \sim 7.2$ could potentially decrease the solution pH to around 5.7. Such a pH change was not observed, however, probably because of the contemporary consumption of H^+ in reaction (2).

It is also possible to calculate a lower limit for the polychromatic quantum yield of $\cdot\text{NO}_2$ generation by INN, under the hypothesis that all $\cdot\text{NO}_2$ reacts with phenol and that the nitration yield of phenol by $\cdot\text{NO}_2$ is unity. In the studied system it is $P_a^{\text{INN}} = 3.42 \times 10^{-7}$ einstein $\text{L}^{-1} \text{s}^{-1}$ and $P_a^{\text{NO}_2^-} = 1.68 \times 10^{-7}$ einstein $\text{L}^{-1} \text{s}^{-1}$. By comparison, 10 mM nitrite alone absorbs 1.87×10^{-7} einstein $\text{L}^{-1} \text{s}^{-1}$. The overall formation rate of the two nitrophenols with INN + nitrite is $(6.7 \pm 0.9) \times 10^{-9} \text{ M s}^{-1}$, to be compared with $(9.8 \pm 0.9) \times 10^{-10} \text{ M s}^{-1}$ in the presence of nitrite alone. The processes induced by nitrite alone would contribute to the formation of the nitrophenols also in the system containing INN, and the corresponding reaction rate is expected to be proportional to the photon flux absorbed by nitrite. Accordingly, the contribution of nitrite photolysis to phenol nitration would be slightly lower in the presence of INN + NO_2^- than with NO_2^- alone. Given these premises, the reaction (1) between excited INN and nitrite in the studied system is expected to contribute $\text{Rate}_{\text{NP}}^{\text{INN}} = (5.8 \pm 1.0) \times 10^{-9} \text{ M s}^{-1}$ to nitrophenol formation, which corresponds to a polychromatic quantum yield $\Phi_{\text{NP}}^{\text{INN}} = \text{Rate}_{\text{NP}}^{\text{INN}} (P_a^{\text{INN}})^{-1} = (1.7 \pm 0.3) \times 10^{-2}$. That would be the lower limit for the polychromatic quantum yield of $\cdot\text{NO}_2$ production by INN under irradiation, $\Phi_{\cdot\text{NO}_2}^{\text{INN}}$, in the presence of 10 mM nitrite. The LFP results (see insert in Fig. 2A) also suggest that 10 mM nitrite is able to completely quench ^3INN . Under such circumstances, practically all ^3INN would react with NO_2^- to yield $\cdot\text{NO}_2$, and $\Phi_{\cdot\text{NO}_2}^{\text{INN}}$ would be independent of $[\text{NO}_2^-]$. In contrast, at very low $[\text{NO}_2^-]$ the reaction with nitrite would scavenge ^3INN to a lesser extent, and $\Phi_{\cdot\text{NO}_2}^{\text{INN}}$ would be directly proportional to $[\text{NO}_2^-]$. Based on these considerations and on the fact that the first-order decay constant of ^3INN without nitrite is $6.0 \times 10^5 \text{ s}^{-1}$, while the second-order rate constant between ^3INN and NO_2^- is $(3.36 \pm 0.28) \times 10^9 \text{ M}^{-1} \text{s}^{-1}$ at pH 6.5, one would get the following trend for $\Phi_{\cdot\text{NO}_2}^{\text{INN}}$ vs. $[\text{NO}_2^-]$:

$$\Phi_{\cdot\text{NO}_2}^{\text{INN}} \geq (1.7 \pm 0.3) \times 10^{-2} \times \frac{(3.36 \pm 0.28) \times 10^9 [\text{NO}_2^-]}{6.0 \times 10^5 + (3.36 \pm 0.28) \times 10^9 [\text{NO}_2^-]} \quad (4)$$

Generation of $\cdot\text{OH}$ by irradiated INN

Brigante and coworkers¹⁵ have shown that excited INN could produce $\cdot\text{OH}$ upon oxidation of water. Moreover, the authors suggested that the reaction of $\text{INN}^{\cdot-}$ with oxygen leads to the formation of the superoxide radical anion ($\text{O}_2^{\cdot-}$), following reaction (5). The radical $\text{O}_2^{\cdot-}$ ($\text{p}K_a = 4.88$) could undergo dismutation to generate hydrogen peroxide (reaction (6)), with a second-order rate constant of $9.7 \times 10^7 \text{ M}^{-1} \text{s}^{-1}$ at pH 6.5.²⁶ H_2O_2 could then be photolysed to $\cdot\text{OH}$ under the irradiation conditions used in this work ($\lambda \geq 300 \text{ nm}$).



A preliminary experiment was performed in order to support this hypothesis. Terephthalic acid (TA) reacts with $\cdot\text{OH}$ leading to the formation of 2-hydroxyterephthalic acid (TAOH), quantifiable via the fluorescence technique.²⁷ Therefore, TA was used as chemical probe to assess the photoformation of $\cdot\text{OH}$ during irradiation of INN. TA ($4.0 \times 10^{-4} \text{ M}$) was irradiated in the presence of INN ($3.5 \times 10^{-5} \text{ M}$) in aerated and argon-saturated solution. The

irradiation wavelength was set to 365 nm (by using a 1000 W xenon lamp coupled with a monochromatic system). From the experimental results (see Fig. 6), a 3-fold decrease of photoformed $\cdot\text{OH}$ moles was estimated in the absence of oxygen, under which conditions reaction (5) would be strongly inhibited. Such a result suggests that both processes (oxidation of water and photolysis of photogenerated H_2O_2) may account for the formation of $\cdot\text{OH}$ in the studied system. However, additional experiments will be required to further test the hypothesis, including the quantification of photogenerated H_2O_2 .

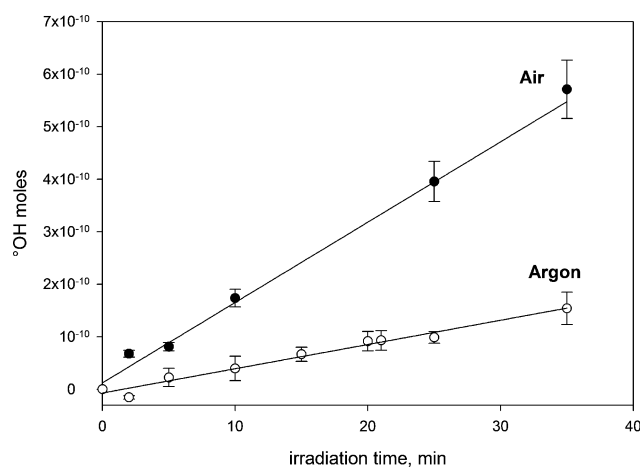


Fig. 6 Time evolution of photoformed $\cdot\text{OH}$ moles upon monochromatic irradiation (365 nm) of $3.5 \times 10^{-5} \text{ M}$ INN + $4.0 \times 10^{-4} \text{ M}$ TA, in aerated and argon-saturated solutions. The experiments were performed at pH 6.5 and $T = 295 \pm 2 \text{ K}$.

Fig. 7 reports the time evolution of phenol upon irradiation of 0.1 mM INN + 4 mM benzene, in aerated solution under the TL 01 lamp. The formation of phenol from benzene is a suitable probe reaction to determine the generation rate of $\cdot\text{OH}$ from irradiated INN, as well as the relevant polychromatic quantum yield.²⁸ To further test the actual formation of $\cdot\text{OH}$, the time evolution of phenol was monitored upon addition of 0.1 M 2-propanol. The initial formation rate of phenol upon irradiation of 0.1 mM

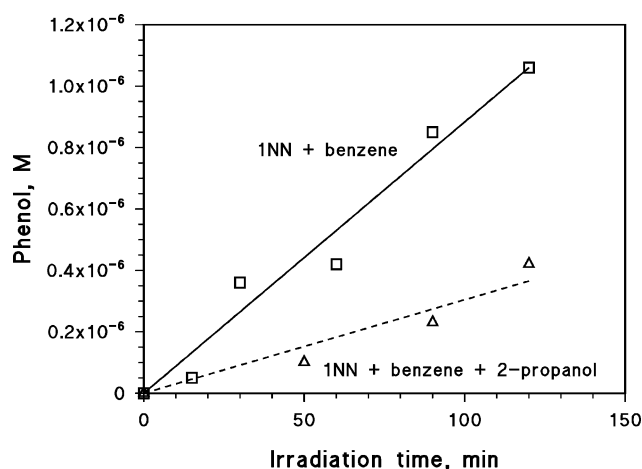


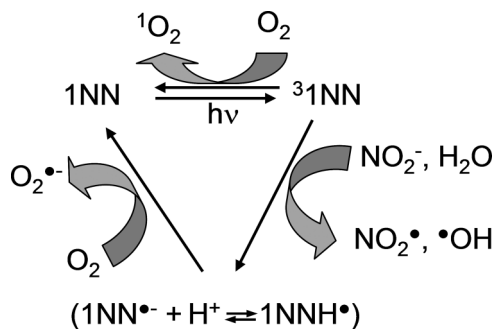
Fig. 7 Time evolution of phenol upon irradiation of 0.1 mM INN + 4 mM benzene, and of 0.1 mM INN + 4 mM benzene + 0.1 M 2-propanol, under the TL 01 lamp at pH 6.5 and in aerated solution.

1NN + 4 mM benzene was $R_{\text{Phenol}} = (1.47 \pm 0.08) \times 10^{-10} \text{ M s}^{-1}$. In the presence of 2-propanol the rate decreased to $(5.07 \pm 0.53) \times 10^{-11} \text{ M s}^{-1}$. Based on the reaction rate constants of benzene and 2-propanol with $\cdot\text{OH}$,²⁹ competition for the hydroxyl radical between 4 mM benzene and 0.1 M 2-propanol should decrease the phenol formation rate to $(2.07 \pm 0.11) \times 10^{-11} \text{ M s}^{-1}$. Therefore, there is a residual $R_{\text{Ph,2Pr}} = (3.00 \pm 0.64) \times 10^{-11} \text{ M s}^{-1}$ that cannot be accounted for by reaction with $\cdot\text{OH}$. A possible explanation could be the direct benzene oxidation by $^3\text{1NN}$: a similar effect has already been observed in the presence of anthraquinone-2-sulfonate under irradiation, which also forms a reactive triplet state.³⁰ Under this hypothesis, in the presence of 1NN + benzene under irradiation the formation rate of phenol that could be accounted for by reaction between benzene and $\cdot\text{OH}$ would be $R' = R_{\text{Phenol}} - R_{\text{Ph,2Pr}} = (1.17 \pm 0.14) \times 10^{-10} \text{ M s}^{-1}$.

Note that the radical $\cdot\text{OH}$ could also react with 1NN and the rate constant is not reported. However, even in the case of a diffusion-controlled reaction, the hydroxyl scavenging by 0.1 mM 1NN compared to 4 mM benzene would introduce a $\sim 5\%$ error that is within the range of experimental uncertainty. The reaction between benzene and $\cdot\text{OH}$ yields phenol with a yield of around 95%.²⁸ Therefore, the formation rate of $\cdot\text{OH}$ by irradiated 1NN can be expressed as $R_{\cdot\text{OH}} = R' (0.95)^{-1} = (1.23 \pm 0.15) \times 10^{-10} \text{ M s}^{-1}$.

The photon flux absorbed by 1NN is $P_a^{1\text{NN}} = \int \lambda p^0(\lambda) \times (1 - 10^{-A_{1\text{NN}}(\lambda)}) d\lambda = 3.60 \times 10^{-7} \text{ einstein L}^{-1} \text{ s}^{-1}$, where $p^0(\lambda)$ is the lamp spectral photon flux density reaching the solution (see Fig. 1) and $A_{1\text{NN}}(\lambda) = \varepsilon_{1\text{NN}}(\lambda)b[1\text{NN}]$, with $b = 0.4 \text{ cm}$ and $[1\text{NN}] = 1.0 \times 10^{-4} \text{ M}$. Therefore, the polychromatic quantum yield of $\cdot\text{OH}$ photogeneration by 1NN under irradiation is $\Phi_{\cdot\text{OH}}^{1\text{NN}} = R_{\cdot\text{OH}}(P_a^{1\text{NN}})^{-1} = (3.42 \pm 0.42) \times 10^{-4}$.

Interestingly, in the presence of nitrite the radicals $\cdot\text{OH}$ generated by 1NN under irradiation could react with NO_2^- and contribute to the photoproduction of $\cdot\text{NO}_2$. Scheme 1 reports the main processes involving 1NN, after radiation absorption, in the presence of H_2O , nitrite and oxygen.



Scheme 1 Proposed reaction pathways and formation of reactive species taking place after radiation absorption by 1NN.

Photonitration of 1NN

First of all, no nitration of 1NN was detected in the presence of HNO_2 in the dark or of $(\text{NH}_4)_2\text{Ce}(\text{NO}_3)_6 + \text{HNO}_3$ under irradiation, the latter yielding $\cdot\text{NO}_3 + \cdot\text{NO}_2$.^{18,31}

Fig. 8 reports the pH trend of the initial transformation rate of 0.1 mM 1NN and of the initial formation rates of 15DNN and 18DNN, upon irradiation with 1 mM NaNO_2 under the TL

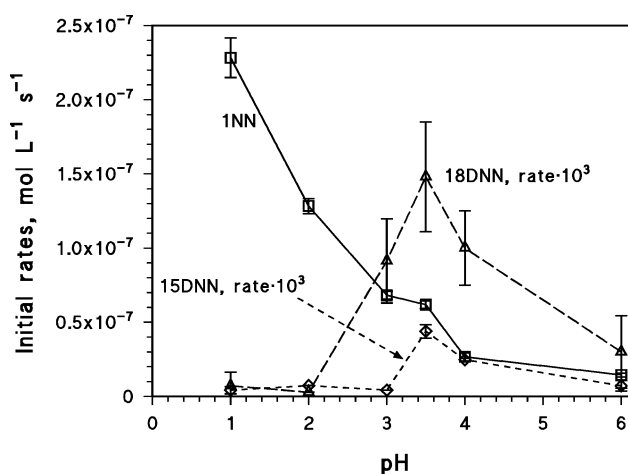


Fig. 8 Initial transformation rate of 1NN and initial formation rates of 15DNN and 18DNN upon UVA irradiation in aerated solution of 0.1 mM 1NN and 1 mM NaNO_2 , as a function of pH, adjusted by addition of HClO_4 .

K05 lamps. The pH was adjusted by addition of HClO_4 . Note that 13DNN was not detected under the adopted irradiation conditions. Some pH increase (up to around 7.5) was observed upon irradiation of the samples at the natural pH (pH 6), possibly because of H^+ consumption in reaction (2). In contrast, the pH variation upon irradiation of the samples acidified with HClO_4 was negligible.

Fig. 8 also shows that the nitration of 1NN into 15DNN and 18DNN takes place with low yield and is maximum around pH 3.5. This is an unusual finding considering that, in most cases, the photonitration processes closely follow the acid–base equilibrium between nitrous acid and nitrite, with a flexus around pH 3.3 (the pK_a of HNO_2).²⁵ Therefore, photonitration is usually more effective under acidic conditions.^{11,32–34} Because of its unusual features, the nitration pathway of 1NN was further studied.

The addition of 0.1 M 2-propanol as $\cdot\text{OH}$ scavenger was able to inhibit significantly the formation of 18DNN and 15DNN at pH 3.5 (see Fig. ESI2†).

Discussion

Photonitration of 1NN

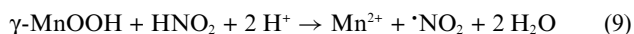
The transformation rate of 1NN with $\text{HNO}_2/\text{NO}_2^-$ under irradiation was higher at low pH. A similar trend was also observed for the rate of the direct phototransformation of 1NN, although the transformation of the substrate was faster in the presence of $\text{HNO}_2/\text{NO}_2^-$ (see Fig. ESI3†). In the absence of nitrite it has been shown that the decay rate constant of $^3\text{1NN}$ is higher at low pH, because of the formation of protonated $^3\text{1NN-H}^+$ that undergoes faster decay compared to $^3\text{1NN}$.^{15,35} In the presence of nitrite/ HNO_2 ($\text{pK}_{a,\text{HNO}_2} \approx 3.3^{25}$), photolysis of these species to yield $\cdot\text{OH}$ could enhance the transformation of 1NN. Note that the photolysis of HNO_2 (reaction (7)) is considerably more efficient than that of nitrite,³⁶ which could contribute to the faster transformation of 1NN at pH 3 compared to pH 6.5. Another process that would contribute to the transformation of 1NN is the reaction between $^3\text{1NN}$ and nitrite/ HNO_2 . This process would be more important at higher pH (see Fig. 4).



As far as the inhibition of 1NN photonitration by 2-propanol is concerned (Fig. ESI2†), the scavenging of $\cdot\text{OH}$ by the alcohol would inhibit the formation of the nitrating agent $\cdot\text{NO}_2$ upon irradiation of nitrite/HNO₂ (see reactions (2), (3), (7), (8)).¹⁸

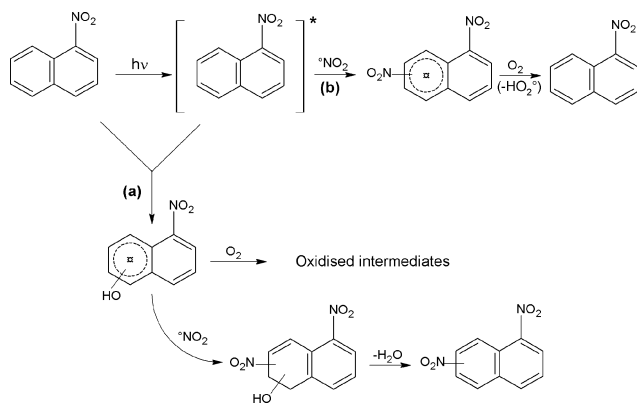


The effect of 2-propanol on the formation of the dinitronaphthalenes is compatible with $\cdot\text{NO}_2$ being involved at some level into the nitration of 1NN. Interestingly, no formation of the dinitronaphthalenes was observed in the presence of $\gamma\text{-MnOOH} + \text{HNO}_2$ in the dark. The Mn (hydr)oxide in acidic solution is able to oxidise HNO₂ to $\cdot\text{NO}_2$:³⁷



In contrast, the dinitronaphthalenes were detected when the system 1NN + $\gamma\text{-MnOOH} + \text{HNO}_2$ was UVA irradiated, suggesting that either (i) nitration involves excited rather than ground-state 1NN, or (ii) it is necessary that reactions (2) and (7) produce $\cdot\text{OH}$ for 1NN to be nitrated.

Interestingly, a significant decrease of the formation of both 18DNN and 15DNN was observed in deoxygenated solution (N₂ atmosphere, see Fig. ESI4†). A nitration pathway that involves $\cdot\text{OH} + \cdot\text{NO}_2$ would be inhibited by oxygen, which would shift the reaction toward the formation of oxygenated/hydroxylated compounds (see pathway (a) in Scheme 2). In contrast, a nitration process directly involving $\cdot\text{NO}_2$ would require oxygen in the second step to abstract a H-atom (see pathway (b) in Scheme 2).

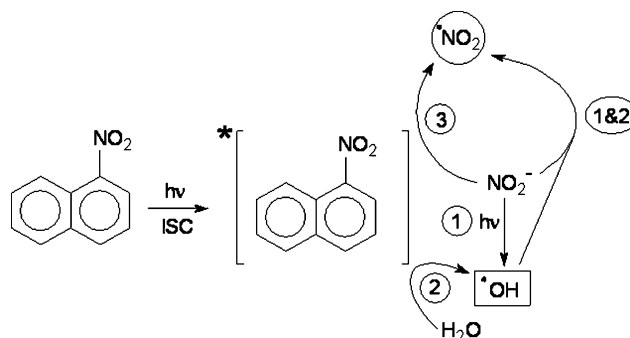


Scheme 2 shows the nitration pathways of 1NN (by $\cdot\text{OH} + \cdot\text{NO}_2$ or $\cdot\text{NO}_2$ alone) that would be compatible with the experimental data reported so far.

Therefore, the inhibition of 1NN photonitration under N₂ atmosphere is consistent with pathway (b), and the nitration of excited 1NN (probably ³1NN) would involve $\cdot\text{NO}_2$ alone. Interestingly, a similar conclusion has been reached for the nitration of the mononitrophenols.¹¹ The second-order rate constant between $\cdot\text{NO}_2$ and the excited triplet states of the mononitrophenols has been estimated, as $7.9 \times 10^7 \text{ M}^{-1} \text{ s}^{-1}$ for 2-nitrophenol and $5.9 \times 10^7 \text{ M}^{-1} \text{ s}^{-1}$ for 4-nitrophenol.³⁸

Generation of $\cdot\text{NO}_2$ by 1NN and nitrite/nitrous acid under irradiation

It was shown before that the photonitration of 1NN would involve $\cdot\text{NO}_2$. The generation of $\cdot\text{NO}_2$ in the studied system can take place by the following processes (see Scheme 3): (1) oxidation of nitrite/nitrous acid by the $\cdot\text{OH}$ radicals photogenerated by their photolysis (reactions (2), (3), (7), (8)); (2) oxidation of nitrite/nitrous acid by $\cdot\text{OH}$ photogenerated by ³1NN; (3) direct oxidation of nitrite/nitrous acid by ³1NN (reaction (1)). Under neutral conditions, nitrite and its (photo)chemistry would strongly prevail over HNO₂. The quantum yield of reaction (2) varies from 0.07 below 300 nm to 0.025 above 350 nm.³⁹ In the studied systems nitrite was irradiated in the presence of 1NN, which also absorbs radiation and can yield $\cdot\text{NO}_2$ with a polychromatic quantum yield $\Phi_{\cdot\text{NO}_2}^{1\text{NN}}$ that is described by eqn (4). In the presence of 1 mM nitrite and 0.1 mM 1NN under the TL K05 lamp, it is $P_a^{\text{NO}_2^-} = 3.76 \times 10^{-7} \text{ einstein L}^{-1} \text{ s}^{-1}$ and $P_a^{1\text{NN}} = 6.88 \times 10^{-6} \text{ einstein L}^{-1} \text{ s}^{-1}$. A reasonable value for the polychromatic photolysis quantum yield of nitrite under the adopted lamp is 0.035,³⁹ which gives $R_{\cdot\text{OH}}^{\text{NO}_2^-} \approx 1.3 \times 10^{-8} \text{ M s}^{-1}$. Nitrite is expected to be the main scavenger of $\cdot\text{OH}$ in the system, thus it would also be $R_{\text{NO}_2}^{\text{NO}_2^-} \approx 1.3 \times 10^{-8} \text{ M s}^{-1}$.



Scheme 3 Processes leading to $\cdot\text{NO}_2$ formation in the studied system. Numbers are referred to the $\cdot\text{NO}_2$ generation pathways as described in the text.

This is to be compared with $R_{\cdot\text{NO}_2}^{1\text{NN}} = \Phi_{\cdot\text{NO}_2}^{1\text{NN}} P_a^{1\text{NN}} \geq (1.0 \pm 0.4) \times 10^{-7} \text{ M s}^{-1}$ (from eqn (4), with $[\text{NO}_2^-] = 10^{-3} \text{ M}$). Finally, $\cdot\text{NO}_2$ could also be produced upon oxidation of nitrite by $\cdot\text{OH}$, photogenerated by ³1NN. Considering that nitrite would scavenge almost all the photogenerated $\cdot\text{OH}$, the formation rate of $\cdot\text{NO}_2$ via this pathway would be equal to the formation rate of $\cdot\text{OH}$ by ³1NN ($R_{\cdot\text{OH}}^{1\text{NN}} = \Phi_{\cdot\text{OH}}^{1\text{NN}} P_a^{1\text{NN}} = (2.4 \pm 0.3) \times 10^{-9} \text{ M s}^{-1}$). By comparing the three pathways it can be seen that the oxidation of nitrite by ³1NN would play the main role toward the formation of $\cdot\text{NO}_2$. The photolysis of nitrite would be less important, while the contribution of $\cdot\text{OH}$ generated by ³1NN would be minor. Note that the photoproduction of $\cdot\text{NO}_2$ by ³1NN + NO₂⁻ would not necessarily enhance 1NN photonitration. Indeed, if the latter process involves ³1NN + $\cdot\text{NO}_2$, the scavenging of ³1NN by nitrite would decrease the steady-state [³1NN], which would compensate for the parallel $\cdot\text{NO}_2$ generation.

The use of polychromatic photolysis quantum yields leads to unavoidable approximations. However, in this case the differences between the estimated rates of the $\cdot\text{NO}_2$ generation processes are equal to or higher than one order of magnitude. Therefore, the

approximations in the rate estimates would not be able to bias the conclusions concerning the rate comparison.

Under acidic conditions, in the presence of 0.1 mM 1NN + 1 mM HNO₂ it would be $P_a^{\text{HNO}_2} = 7.6 \times 10^{-7}$ einstein L⁻¹ s⁻¹, $P_a^{\text{1NN}} = 6.8 \times 10^{-6}$ einstein L⁻¹ s⁻¹, and $\Phi_{\text{OH}}^{\text{HNO}_2} = 0.35$.³⁹ Therefore, one obtains $R_{\text{OH}}^{\text{HNO}_2} = 2.7 \times 10^{-7}$ M s⁻¹. Nitrous acid would be the main •OH scavenger in the system, thus $R_{\text{NO}_2}^{\text{HNO}_2} \approx 2.7 \times 10^{-7}$ M s⁻¹. Note that the photoproduction of •NO₂ by HNO₂ is much more efficient compared to that by nitrite. The generation of •NO₂ by ³1NN is expected to decrease under acidic conditions (see Fig. 4), thus HNO₂ photolysis could be the main source of •NO₂ at pH ≤ 3.

Fig. 8 shows that the formation of the dinitronaphthalenes is maximum at pH 3.5. At higher pH, the formation of •NO₂ would be decreased because the photolysis of nitrite is less efficient compared to that of HNO₂. That would inhibit the photonitration of 1NN. Moreover, the steady-state [³1NN] is expected to decrease with increasing pH, because the reaction rate constant between ³1NN and nitrite increases with pH (Fig. 4). As far as 1NN photonitration (probably involving ³1NN + •NO₂) is concerned, the scavenging of ³1NN by nitrite would compensate for the generation of •NO₂ by the same reaction.

At low pH values, the nitration pathways might be modified by the presence of the protonated triplet state, ³1NN-H⁺.^{14,15} To account for the inhibition of 1NN photonitration below pH 3.5, one has to consider that nitration is probably involving reaction between ³1NN and •NO₂, and that both ³1NN and ³1NN-H⁺ would likely react with •NO₂. Under the hypothesis that only the reaction of •NO₂ with ³1NN produces the dinitronaphthalenes, if ³1NN-H⁺ reacts with •NO₂ much faster than ³1NN, depletion of •NO₂ without production of 15DNN or 18DNN could be operational in the presence of ³1NN-H⁺. As a consequence, the formation rate of the dinitronaphthalenes would be decreased.

Atmospheric significance

The triplet state of 1NN is able to react with O₂ (rate constant $(1.95 \pm 0.05) \times 10^9$ M⁻¹ s⁻¹),¹⁵ but also with dissolved anions such as bromide $((7.5 \pm 0.2) \times 10^8$ M⁻¹ s⁻¹)¹⁵ and nitrite $((3.36 \pm 0.28) \times 10^9$ M⁻¹ s⁻¹ at pH 6.5) (this work) (see Scheme 1). In aerated solution the concentration of O₂ can be around 0.3 mM, bromide can reach up to 20 μM in sea-salt aerosol,⁴⁰ nitrite up to 4 μM in rain⁴¹ and up to 60 μM in fog⁴² (pH around 6–6.5 in both cases). With 4 μM nitrite and the cited O₂ and bromide levels, 95% of ³1NN would be scavenged by O₂ and 2–3% each by bromide and nitrite. In contrast, 60 μM nitrite would scavenge around 25% of ³1NN. These data suggest that nitrite could be an important scavenger of ³1NN in fog water in polluted areas. The reaction would contribute to the transformation of 1NN and would yield •NO₂ that is a nitrating agent in the aqueous phase.^{11,32}

It is also possible to compare the formation of •OH and of •NO₂ by ³1NN. The former process has quantum yield $\Phi_{\text{OH}} \sim 3.4 \times 10^{-4}$, and a lower limit for Φ_{NO_2} is given by eqn (4). The polychromatic quantum yield values are approximated but they can be useful to have a rough comparison between the two processes. From the values of Φ_{OH} and Φ_{NO_2} it can be foreseen that [NO₂⁻] ≥ 4 μM would ensure a prevalence of •NO₂ generation over that of •OH in the presence of excited 1NN. An even lower [NO₂⁻] would be sufficient if the quantum yield of •NO₂ generation is higher than

foreseen by eqn (4), but a 4 μM nitrite level is well within the range of fog waters⁴² and is also significant for rainwater in polluted areas.⁴¹

Conclusions

The excited triplet state of 1NN (³1NN) is able to oxidise nitrite to •NO₂. The second-order rate constant $k^{\text{31NN,NO}_2}$ varies from $(3.56 \pm 0.11) \times 10^8$ M⁻¹ s⁻¹ at pH 2.0 to $(3.36 \pm 0.28) \times 10^9$ M⁻¹ s⁻¹ at pH 6.5. The polychromatic quantum yield of •NO₂ photogeneration by 1NN in neutral solution, $\Phi_{\text{NO}_2}^{\text{1NN}}$, is described by eqn (4) and is valid in the wavelength interval of 300–440 nm. In neutral solution, the oxidation of nitrite by ³1NN is a competitive •NO₂ source compared to the photolysis of nitrite. Irradiated 1NN is also able to produce •OH via oxidation of water and/or via reactions (5) and (6) followed by the photolysis of H₂O₂, with a polychromatic quantum yield $\Phi_{\text{OH}}^{\text{1NN}} = (3.42 \pm 0.42) \times 10^{-4}$ between 300 and 440 nm. The irradiation of 1NN in the presence of nitrite yields the dinitronaphthalene isomers 15DNN and 18DNN, and the photonitration pathway is likely to involve reaction between excited 1NN (possibly ³1NN) and •NO₂. The photonitration of 1NN is maximum around pH 3.5. At higher pH the formation rate of •NO₂ would be lower because the photolysis of nitrite is less efficient compared to that of HNO₂. Moreover, the production of •NO₂ by ³1NN + nitrite (reaction (1)) could not enhance photonitration because of the parallel scavenging of ³1NN, which is likely involved into the nitration process. At lower pH, the reaction between ³1NN and •NO₂ is probably replaced by other processes (e.g. reaction between ³1NN-H⁺ and •NO₂) that do not yield the dinitronaphthalenes.

Overall, nitrite can be an important scavenger of ³1NN at the tens μM [NO₂⁻] levels that can be found in fog water in polluted areas

Acknowledgements

DV, VM and CM acknowledge financial support by PNRA-Progetto Antartide and MIUR-PRIN 2007 (2007L8Y4NB, Area 02, project n° 36). The work of PRM in Torino was supported by a Marie Curie International Incoming Fellowship (IIF), under the FP7-PEOPLE programme (contract n° PIIF-GA-2008-219350, project PHOTONIT). MB, TC and GM acknowledge the support of the INSU-CNRS through the projects LEFE-CHAT and ORE BEAM and Conseil Regional d'Auvergne for PhD grant provided to TC.

Notes and references

- 1 A. Delgado Rodriguez, R. Ortiz Marttelo, U. Graf, R. Villalobos, Pietrini and S. Gomez Arroyo, Genotoxic activity of environmentally important polycyclic aromatic hydrocarbons and their nitro derivatives in the wing spot test of *Drosophila melanogaster*, *Mutat. Res.-Genet. Toxicol.*, 1995, **341**, 235–247.
- 2 R. R. Dihl, M. S. Bereta, V. S. do Amaral, M. Lehmann, M. L. Reguly and H. H. R. de Andrade, Nitropolycyclic aromatic hydrocarbons are inducers of mitotic homologous recombination in the wing-spot test of *Drosophila melanogaster*, *Food Chem. Toxicol.*, 2008, **46**, 2344–2348.
- 3 M. Dimashki, S. Harrad and R. M. Harrison, Measurements of nitro-PAH in the atmospheres of two cities, *Atmos. Environ.*, 2000, **34**, 2459–2469.
- 4 R. Atkinson, S. M. Aschmann, J. Arey, B. Zielinska and D. Schuetzle, Gas-phase atmospheric chemistry of 1-nitronaphthalene

- and 2-nitronaphthalene and 1,4-naphthoquinone, *Atmos. Environ.*, 1989, **23**, 2679–2690.
- 5 A. Feilberg, R. M. Kamens, M. R. Strommen and T. Nielsen, Modeling the formation, decay, and partitioning of semivolatile nitro-polycyclic aromatic hydrocarbons (nitronaphthalenes) in the atmosphere, *Atmos. Environ.*, 1999, **33**, 1231–1243.
 - 6 N. Nishino, R. Atkinson and J. Arey, Formation of nitro products from the gas-phase OH radical-initiated reactions of toluene, naphthalene, and biphenyl: Effect of NO concentration, *Environ. Sci. Technol.*, 2008, **42**, 9203–9209.
 - 7 N. V. Heeb, P. Schmid, M. Kohler, E. Gujer, M. Zennegg, D. Wenger, A. Wichser, A. Ulrich, U. Gfeller, P. Honegger, K. Zeyer, L. Emmenegger, J. L. Petermann, J. Czerwinski, T. Mosimann, M. Kasper and A. Mayer, Impact of low- and high-oxidation diesel particulate filters on genotoxic exhaust constituents, *Environ. Sci. Technol.*, 2010, **44**, 1078–1084.
 - 8 P. T. Phouongphouang and J. Arey, Rate constants for the photolysis of the nitronaphthalenes and methyl-nitronaphthalenes, *J. Photochem. Photobiol., A*, 2003, **157**, 301–309.
 - 9 M. Vincenti, V. Maurino, C. Minero and E. Pelizzetti, Detection of nitro-substituted polycyclic aromatic hydrocarbons in the Antarctic airborne particulate, *Int. J. Environ. Anal. Chem.*, 2001, **79**, 257–272.
 - 10 C. Minero, V. Maurino, D. Borghesi, E. Pelizzetti and D. D. Vione, An overview of possible processes able to account for the occurrence of nitro-PAHs in Antarctic particulate matter, *Microchem. J.*, 2010, **96**, 213–217.
 - 11 D. Vione, V. Maurino, C. Minero and E. Pelizzetti, Aqueous atmospheric chemistry: Formation of 2,4-dinitrophenol upon nitration of 2-nitrophenol and 4-nitrophenol in solution, *Environ. Sci. Technol.*, 2005, **39**, 7921–7931.
 - 12 J. S. Zugazagoitia, C. X. Almora-Diaz and J. Peon, Ultrafast inter-system crossing in 1-nitronaphthalene. An experimental and computational study, *J. Phys. Chem. A*, 2008, **112**, 358–365.
 - 13 J. S. Zugazagoitia, S. Collado-Fregoso, E. F. Plaza-Medina and J. Peon, Relaxation in the triplet manifold of 1-nitronaphthalene observed by transient absorption spectroscopy, *J. Phys. Chem. A*, 2009, **113**, 805–810.
 - 14 L. J. A. Martins, M. M. M. M. Fernandez, T. J. Kemp, S. J. Formosinho and J. S. Branco, Interaction of halide and pseudohalide ions with the triplet state of 1-nitronaphthalene. Effect of acidity: a flash photolysis study, *J. Chem. Soc., Faraday Trans.*, 1991, **87**, 3617–3624.
 - 15 M. Brigante, T. Charbouillot, D. Vione and G. Mailhot, Photochemistry of 1-nitronaphthalene: A potential source of singlet oxygen and radical species in atmospheric waters, *J. Phys. Chem. A*, 2010, **114**, 2830–2836.
 - 16 S. Net, L. Nieto-Gligorovski, S. Gligorovski, B. Temime-Roussel, S. Barbat, Y. G. Lazarou and H. Wortham, Heterogeneous light-induced ozone processing on the organic coatings in the atmosphere, *Atmos. Environ.*, 2009, **43**, 1683–1692.
 - 17 I. Grgic, L. I. Nieto-Gligorovski, B. Temime-Roussel, S. Gligorovski and H. Wortham, Light induced multiphase chemistry of gas-phase ozone on aqueous pyruvic and oxalic acids, *Phys. Chem. Chem. Phys.*, 2010, **12**, 698–707.
 - 18 J. Mack and J. R. Bolton, Photochemistry of nitrite and nitrate in aqueous solution: a review, *J. Photochem. Photobiol., A*, 1999, **128**, 1–13.
 - 19 G. Brauer, (Ed.), *Handbook of preparative inorganic chemistry*, Vol. 2, 2nd ed., Academic Press, NY, London, 1963.
 - 20 H. J. Kuhn, S. E. Braslavsky and R. Schmidt, Chemical actinometry, *Pure Appl. Chem.*, 2004, **76**, 2105–2146.
 - 21 A. Treinin and E. Hayon, Absorption spectra and reaction kinetics of NO₂, N₂O₃ and N₂O₄ in aqueous solution, *J. Am. Chem. Soc.*, 1970, **92**, 5821–5828.
 - 22 S. Chiron, C. Minero and D. Vione, Occurrence of 2,4-dichlorophenol and of 2,4-dichloro-6-nitrophenol in the Rhone River Delta (Southern France), *Environ. Sci. Technol.*, 2007, **41**, 3127–3133.
 - 23 S. Chiron, L. Comoretto, E. Rinaldi, V. Maurino, C. Minero and D. Vione, Pesticide by-products in the Rhone delta (Southern France). The case of 4-chloro-2-methylphenol and of its nitroderivative, *Chemosphere*, 2009, **74**, 599–604.
 - 24 S. E. Braslavsky, Glossary of terms used in Photochemistry 3rd Edition (IUPAC Recommendations 2006), *Pure Appl. Chem.*, 2007, **79**, 293–465.
 - 25 A. E. Martell, R. M. Smith and R. J. Motekaitis, *Critically selected stability constants of metal complexes database*, version 4.0, 1997.
 - 26 B. H. J. Bielski, D. E. Cabelli, R. L. Arudi and A. B. Ross, Reactivity of HO₂/O₂[•] radicals in aqueous solution, *J. Phys. Chem. Ref. Data*, 1985, **14**, 1041–110.
 - 27 X. Fang, G. Mark and C. von Sonntag, OH radical formation by ultrasound in aqueous solutions. I. The chemistry underlying the terephthalate dosimeter, *Ultrason. Sonochem.*, 1996, **3**, 57–63.
 - 28 K. Takeda, H. Takedoi, S. Yamaji, K. Ohta and H. Sakugawa, Determination of hydroxyl radical photoproduction rates in natural waters, *Anal. Sci.*, 2004, **20**, 153–158.
 - 29 G. V. Buxton, C. L. Greenstock, W. P. Helman and A. B. Ross, Critical review of rate constants for reactions of hydrated electron, hydrogen atoms and hydroxyl radicals (•OH/•O[–]) in aqueous solution, *J. Phys. Chem. Ref. Data*, 1988, **17**, 513–886.
 - 30 D. Vione, M. Ponzio, D. Bagnus, V. Maurino, C. Minero and M. E. Carloti, Comparison of different probe molecules for the quantification of hydroxyl radicals in aqueous solution, *Environ. Chem. Lett.*, 2008, **8**, 95–100.
 - 31 H. Herrmann, M. Exner and R. Zellner, The absorption spectrum of the nitrate (•NO₃) radical in aqueous solution, *Ber. Bunsenges. Phys. Chem.*, 1991, **95**, 598–604.
 - 32 D. Vione, V. Maurino, C. Minero and E. Pelizzetti, Nitration and photolysis of naphthalene in aqueous systems, *Environ. Sci. Technol.*, 2005, **39**, 1101–1110.
 - 33 D. Vione, C. Minero, F. Housari and S. Chiron, Photoinduced transformation processes of 2,4-dichlorophenol and 2,6-dichlorophenol on nitrate irradiation, *Chemosphere*, 2007, **69**, 1548–1554.
 - 34 C. Minero, F. Bono, F. Rubertelli, D. Pavino, V. Maurino, E. Pelizzetti and D. Vione, On the effect of pH in aromatic photolysis upon nitrate photolysis, *Chemosphere*, 2007, **66**, 650–656.
 - 35 W. Trotter and A. C. Testa, Photoreduction of 1-nitronaphthalene by protonation in the excited state, *J. Phys. Chem.*, 1970, **74**, 845–847.
 - 36 T. Arakaki, T. Miyake, T. Hirakawa and H. Sakugawa, pH dependent photoformation of hydroxyl radical and absorbance of aqueous-phase N(III) (HNO₂ and NO₂[–]), *Environ. Sci. Technol.*, 1999, **33**, 2561–2565.
 - 37 D. Vione, V. Maurino, C. Minero and E. Pelizzetti, Phenol nitration upon oxidation of nitrite by Mn(III,IV) (hydr)oxides, *Chemosphere*, 2004, **55**, 941–949.
 - 38 D. Vione, V. Maurino, C. Minero, M. Duncianu, R. I. Olariu, C. Arsene, M. Sarakha and G. Mailhot, Assessing the transformation kinetics of 2- and 4-nitrophenol in the atmospheric aqueous phase. Implications for the distribution of both nitroisomers in the atmosphere, *Atmos. Environ.*, 2009, **43**, 2321–2327.
 - 39 M. Fischer and P. Warneck, Photodecomposition of nitrite and undissociated nitrous acid in aqueous solution, *J. Phys. Chem.*, 1996, **100**, 18749–18756.
 - 40 M. Neal, C. Neal, H. Wickham and S. Harman, Determination of bromide, chloride, fluoride, nitrate and sulfate by ion chromatography: comparisons of methodologies for rainfall, cloud water and river waters at the Plynlimon catchments of mid-Wales, *Hydrol. Earth Syst. Sci.*, 2007, **11**, 294–300.
 - 41 A. Albinet, C. Minero and D. Vione, Photochemical generation of reactive species upon irradiation of rainwater: Negligible photoactivity of dissolved organic matter, *Sci. Total Environ.*, 2010, **408**, 3367–3373.
 - 42 C. Anastasio and K. G. McGregor, Chemistry of fog waters in California's Central Valley: 1. In situ photoformation of hydroxyl radical and singlet molecular oxygen, *Atmos. Environ.*, 2001, **35**, 1079–1089.